

# OBSERVATIONS ON INSTABILITIES OF CAVITATING INDUCERS

by

David Braisted and Christopher Brennen

California Institute of Technology  
Pasadena, California, 91125

## Introduction

Hydraulic systems involving cavitating turbomachines are known to be susceptible to instabilities at certain critical operating conditions. Two distinct classes of cavitating inducer instabilities have been reported in the literature (Refs. 1-6). The purpose of this note is to report on some preliminary observations of these phenomena.

The experiments were performed in the Dynamic Pump Test Facility (DPTF) at the California Institute of Technology (Refs. 7,8). Results will be presented for two different inducers operating at different flow coefficients,  $\Phi$  ( $\Phi$  = mean axial velocity/inducer tip velocity -  $U_a/U_{Tip}$ ) and cavitation numbers,  $\sigma$  ( $\sigma = (p_1 - p_v) / \frac{1}{2} \rho U_{Tip}^2$ ; where  $p_1$ ,  $p_v$  are the inlet and vapor pressures, and  $\rho$  is the liquid density). In general, the instabilities occurred just before head breakdown. After head breakdown, the system tended to become stable again, although there were some indications of a second region of instability at very small cavitation numbers.

Impeller IV is a quarter scale model of the Low Pressure Oxidizer Turbo-Pump (LPOTP) of the space shuttle main engine (Refs. 7,8). The cavitation performance of this impeller is presented in Figure 1. Some of the mean operating states for which large, constant amplitude oscillations occurred in all the pressures and mass flow rates are indicated by stars. The cavitation in each of the blade passages oscillated in unison. This unstable behavior is termed auto-oscillation. The frequency of the auto-oscillations ranged from 28 to 35 Hz. As might be expected, there does exist a marginal region of operation for which the auto-oscillations have a time varying amplitude. These non-steady oscillations occurred as sporadic bursts of auto-oscillation. It was this feature that makes the boundaries of the auto-oscillation region difficult to define.

In addition to the auto-oscillation observations on Impeller IV, two instances of "rotating cavitation" were observed and are labeled by boxes in Figure 1. The presence of rotating cavitation was determined by means of a stroboscope slaved to the rotational speed of the inducer. Rotating cavitation appeared as a non-stationary cavitation patterns which rotated with respect to the "fixed" inducer. (More recent testing has also revealed the existence of a stationary form of rotating cavitation sometimes referred to as alternate blade cavitation.) The large amplitude disturbances in the upstream pressure and mass flow rates which characterized auto-oscillation were not observed during rotating cavitation. This suggests the rotating cavitation is most intimately associated with the dynamic characteristics of the cavitating inducer itself irrespective of the hydraulic system in which it resides.

## System Effects on Auto-Oscillation

Before proceeding with the results for the second impeller, it is necessary to discuss the unsteady, dynamic characteristics of the hydraulic system. In the context of a linear lumped parameter model, the

characteristics of the upstream and downstream portions of the system can be thought of in terms of an impedance (see Figure 3). These complex, frequency dependent system impedances were determined experimentally from measurements of the fluctuating mass flow rates and pressure differences by external excitation of the system over a range of frequencies from 0 to 50 Hz. As one familiar example, an increase in the flow coefficient, accomplished by opening a throttle valve in the discharge line, resulted in a decrease in the real or resistive part of the downstream system impedance. During testing on Impeller IV, it was observed that the time varying oscillations could be suppressed by redistributing the total hydraulic system resistance from the downstream to the upstream portion of the circuit. This indicates that auto-oscillation is dependent upon and quite sensitive to the dynamic characteristics of the entire hydraulic system.

The second impeller tested, Impeller V, is a three bladed, 9° helical inducer (Refs. 7,8). During cavitation performance testing of this inducer, both the constant amplitude and the sporadic types of auto-oscillation were encountered. Two cavitation numbers ( $\sigma = 0.045$  and  $\sigma = 0.018$ ) at which the auto-oscillation was readily repeatable were selected and the behavior as the flow coefficient was changed is presented in Figure 2.

At the cavitation number of 0.045, the cavitation in the inducer was extensive but breakdown had not been reached. The data taken at this cavitation number indicated that an increase in the downstream system impedance resulted in a transition from the constant amplitude to the time varying amplitude form of auto-oscillation. As the flow coefficient was decreased from 0.097 to 0.086, the frequency of the continuous auto-oscillation decreased from 31 to 24 Hz. Simultaneously, the magnitude of the downstream pressure fluctuations decreased by a factor of about 2. For flow coefficients less than 0.086, the auto-oscillation was characterized by alternating periods of larger and smaller amplitudes. The frequency of the oscillation remained relatively constant at 25 Hz. The downstream pressure fluctuation amplitude was approximately an order of magnitude smaller than those before transition. It was also observed that the oscillations in the cavitating backflow were more pronounced under these conditions.

At the cavitation number of 0.018, photographs of Impeller V indicated that the inducer was operating well into breakdown. The observed instability was of the constant amplitude type similar to that at the cavitation number of 0.045. The frequency of the oscillations was 15 Hz. There were virtually no fluctuations in the upstream pressure, whereas the magnitude of the downstream pressure fluctuation was comparable to that at the higher cavitation number.

Another parameter of interest was the effect of variations in the air bladder volume. An air bladder was used in the DPTF to isolate the upstream and downstream portions of the closed system, and it acted dynamically as a capacitor to ground (see Figure 3). It was observed that the frequency of the auto

oscillation and the amplitude of the pressure and mass flow rates remained constant for all bladder volumes or compliances. The importance of this result will become apparent in the discussion to follow.

An additional set of experiments demonstrated that the frequency,  $\Omega$ , of the auto-oscillation scaled with the rotational speed for the inducer. In other words, the dimensionless frequency,  $\omega$ , defined by  $\omega = \Omega H / U_{\text{Tip}}$  ( $H$  = blade tip spacing) remained constant and the rotational speed was varied. It was also noted that the amplitude of the downstream pressure fluctuations decreased monotonically as the rotational speed was reduced.

### Discussion

The dynamic characteristics of both the cavitating inducer and the hydraulic system have been combined in a linear stability analysis. Small amplitude, linear dynamic behavior of the inducer can be represented by a transfer function which relates the fluctuating inlet total pressure,  $h_1$ , and mass flow rate,  $m_1$ , to the same quantities at discharge,  $h_2$  and  $m_2$ . The pump transfer function,  $[Z]$ , is defined as follows (Refs. 7, 8, 9, 10):

$$\begin{bmatrix} h_2 - h_1 \\ m_2 - m_1 \end{bmatrix} = \begin{bmatrix} Z_{11} & Z_{12} \\ Z_{21} & Z_{22} \end{bmatrix} \begin{bmatrix} h_1 \\ m_1 \end{bmatrix} \quad (1)$$

The transfer function is necessarily a function of the mean operating state as well as the frequency,  $\Omega$ .

Figure 3 indicates the model of the DPTF used in this analysis. If the circuit were broken at the point Z and if the fluctuating flow rates  $m_3$  and  $m_4$  on either side of this point X are equated, the following relation is obtained:

$$\frac{P_4}{P_3} = \frac{Z_{21}(Z_{12} - I_D) - Z_{22}(1 + Z_{11})}{(Z_{21}I_U - Z_{22}) + j\omega CT} \quad (2)$$

where

$$T = (1 + Z_{11})I_U + (1 + Z_{22})I_D - I_U I_D Z_{21} - Z_{12}$$

In other words, if a pressure amplifier with a gain given by Eqn. (2) was inserted at the point X, the system would be neutrally stable. But since the compliance,  $C$ , of the air bladder is very large, the term  $j\omega CT$  dominates the relation (The experimental result that the auto-oscillation phenomena was not affected by variations in the compliance of the air bladder confirms that this is a reasonable approximation.). Then, Eqn. (2) requires that  $T$  must vanish for the system to be neutrally stable. We have evaluated  $T$  for all possible combinations of the experimentally determined system impedances and experimentally determined transfer functions of Impellers IV and V (Refs. 7, 8, 9). An example of a phase plane plot of  $T$  for Impeller IV and various combinations of system impedances is presented in Figure 4. In this case, the system was stable. For a given pump transfer function and system impedances, a generalized stability margin,  $\beta$ , is defined as the distance of closest approach to the origin in the  $T$  phase plane (as indicated for the line D in Fig. 4). However, for the given operating state of the transfer function, the pump operates with a specific total resistance given by  $2\Psi/\Phi$ ; thus interpolation was necessary to obtain the stability margins of this operating state for several distributions of the same total resistance.

It transpired that, for all of the available transfer functions, the frequency with the smallest stability margin was between 28 and 35 Hz. This agrees well with our observations. Another feature of the phase plane plot of  $T$  is the marked variation with the

various system impedance combinations. Suppression of auto-oscillation by changes in the system parameters is thus confirmed analytically.

An analysis of rotating cavitation does not exist, to our knowledge, as yet. There are indications in the literature (Refs. 1, 2), however, that rotating cavitation tends to occur when the inducer is lightly loaded (small angles of attack).

### Conclusions

Though further experimental and theoretical work remains to be done, the results of the stability analyses are in qualitative agreement with the observations of auto-oscillation. Indeed, the fact that a linear analysis appears useful in predicting the onset of large amplitude non-linear limit cycle oscillations is valuable.

### Acknowledgments

This investigation is part of an ongoing research program funded under NASA Contract NAS 8-29313. The authors are grateful to the George Marshall Space Flight Center, Huntsville, Alabama for this support. The junior member of this partnership is also grateful to NSF which has supported his research activities at Caltech by means of a Graduate Fellowship.

### References

1. Acosta, A. J., "An Experimental Study of Cavitating Inducers", Proc. of Second ONR Symposium on Naval Hydrodynamics, August 25-29 (ACR-38), 1958.
2. Kamijo, K., Shimura, T. and Watanabe, M., "An Experimental Investigation of Cavitating Inducer Instability", ASME, 77-WA/FE-14, 1977.
3. Young, W. E., Murphy, R., and Reddecliff, J. M., "Study of Cavitating Inducer Instabilities", Pratt and Whitney Aircraft, Florida Research and Development, Rept. PWA FR-5131, August 31, 1972.
4. Badowski, H. R., "An Explanation for Instability in Cavitating Inducers", ASME Cavitation Forum, 1969, pp 38-40.
5. Sack, L. E. and Nottage, H. B., "System Oscillations Associated with Cavitating Inducers", J. Basic Engr., Vol. 87, Series D, No. 4, 1965, pp 917-925.
6. Natazon, M. S., Bal'tsev, N. I., Bazhanov, V. V., and Leydervarger, M. R., "Experimental Investigation of Cavitation-Induced Oscillation of Helical Inducers", Fluid Mechanics, Soviet Res., Vol. 3, No. 1, 1974, pp 38-45.
7. Ng, S. L., "Dynamic Response of Cavitating Turbomachines", PhD Thesis, 1976, California Institute of Technology, Pasadena, California, (Rept. E184.1 Div. of Eng. and App. Sci., C.I.T., August 1976).
8. Ng, S. L. and Brennen, C., "Experiments on the Dynamic Behavior of Cavitating Pumps", paper submitted to J. of Fluids Engr., 1978.
9. Brennen, C., "The Unsteady, Dynamic Characterization of Hydraulic Systems with Emphasis on Cavitation and Turbomachines", paper presented at the joint IAHR-ASME-ASCE Symposium on Design and Operation of Fluid Machinery, Fort Collins, Colorado, June 1978.
10. Brennen, C. and Acosta, A. J., "The Dynamic Transfer Function for a Cavitating Inducer", ASME, 75-WA/FE-16, 1975.

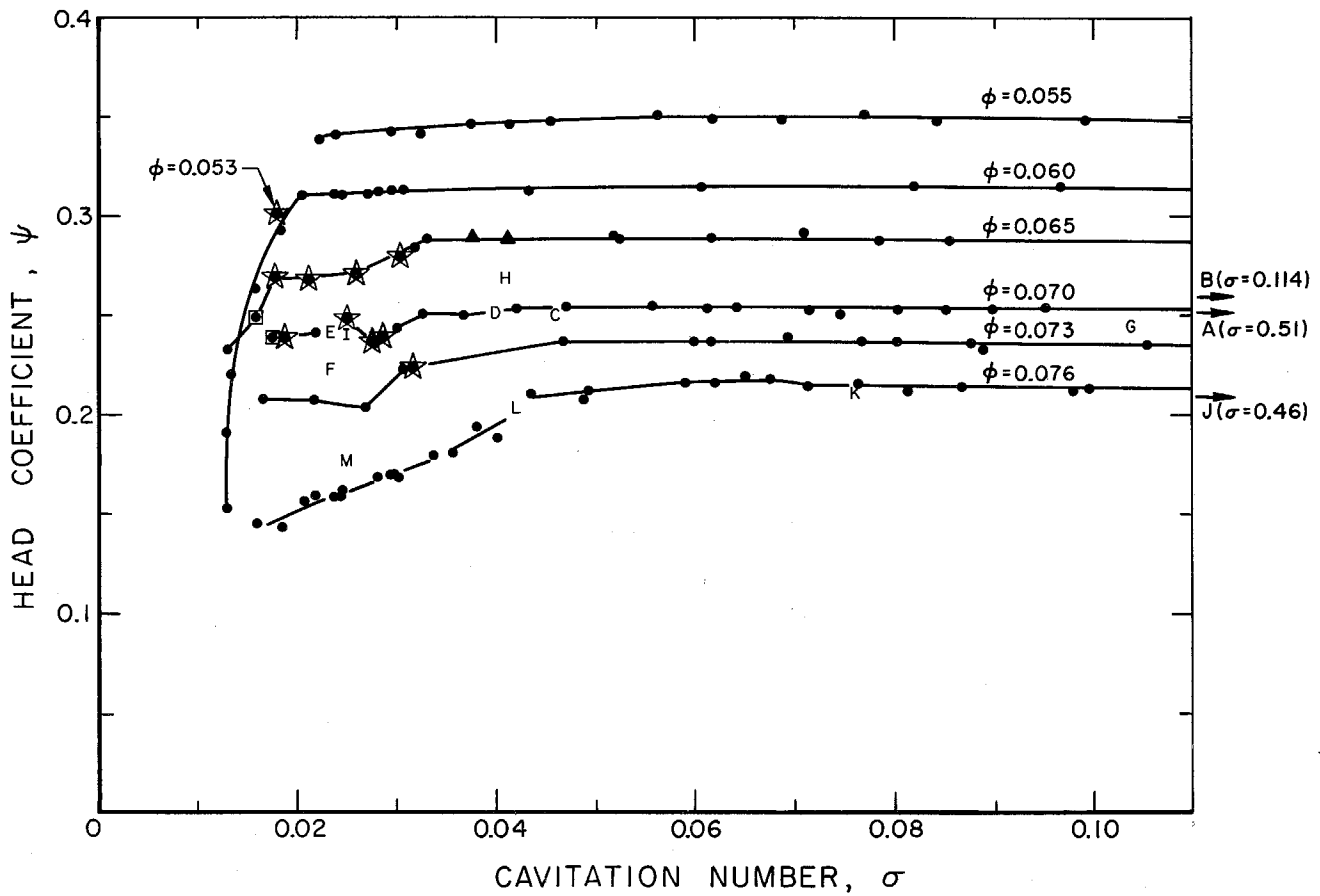


FIGURE 1. Cavitation Performance of Impeller IV at 9000 RPM. The operating conditions for which continuous amplitude auto-oscillation was observed are indicated by  $\star$ , sporadic by  $\blacktriangle$ ; and those for which rotating cavitation occurred by  $\blacksquare$ . Operating points at which dynamic transfer functions for this inducer are available are labeled A, B, ..., M. The head coefficient,  $\Psi$ , is defined by  $\Psi = \Delta p / \frac{1}{2} \rho U_{TIP}^2$ , where  $\Delta p$  is the head rise across the pump.

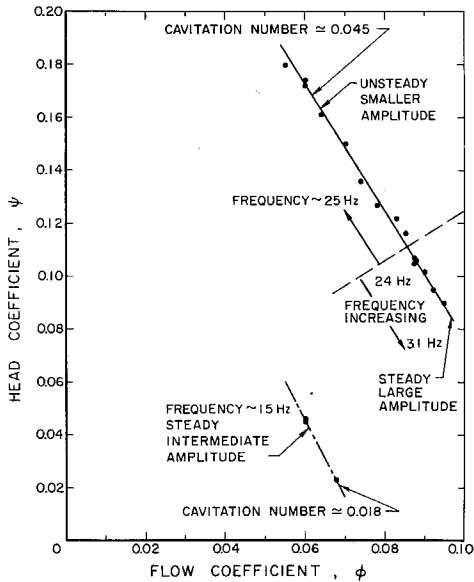


Figure 2. Auto-Oscillation of Impeller V.

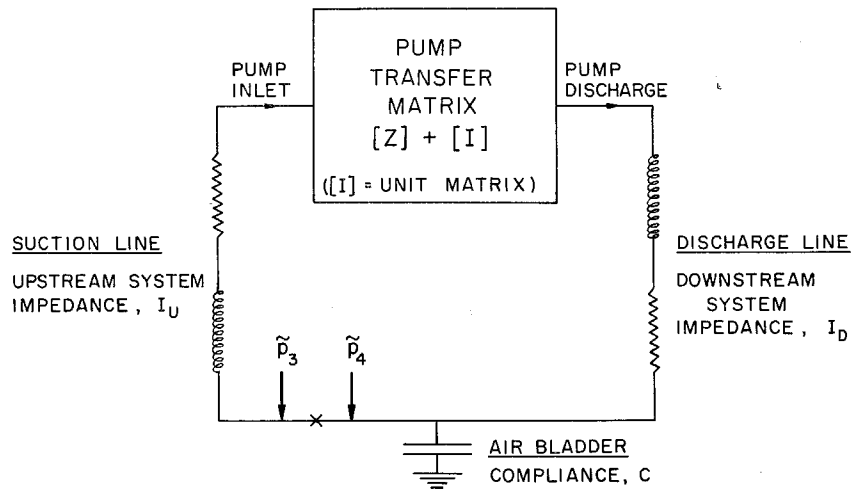


FIGURE 3. Lumped Parameter Model of Hydraulic System for Auto-Oscillation Analysis.

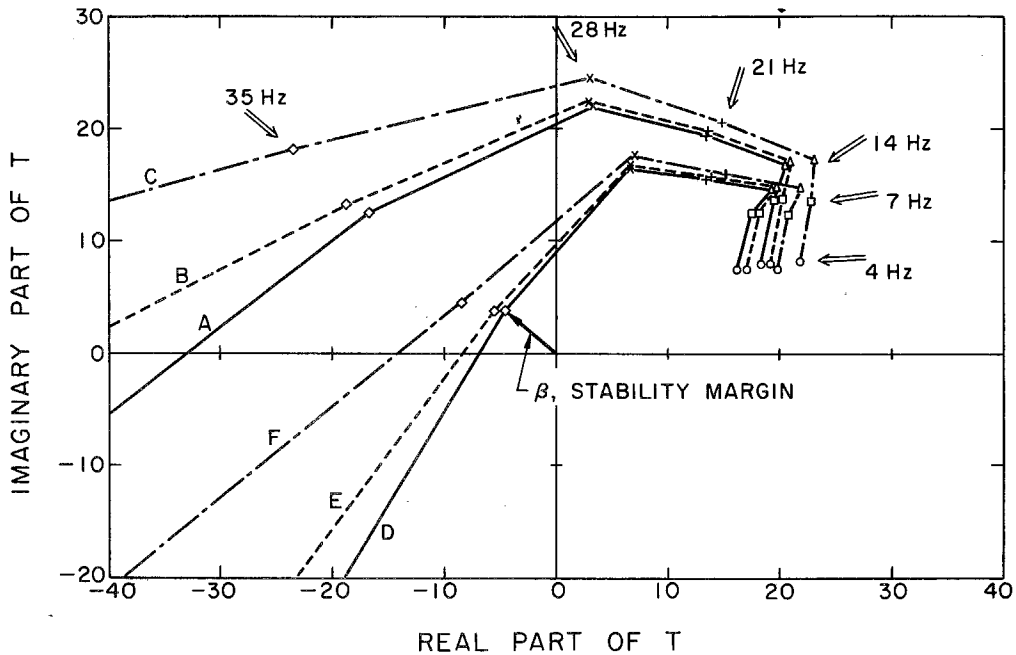


FIGURE 4. Phase Plane Plot of  $T$  for the Transfer Matrix of Impeller IV at operating point, B (see Fig. 1). Points for different frequencies are shown on the graph. The six different lines are for different combinations of upstream and downstream impedance. The sets (A, B, C) and (D, E, F) are for different downstream impedances and increasing upstream impedances.